

## Analysis of the Chari Baguirmi piezometric depression setting up (East of lake Chad) using a coupled sedimentology - geochemistry approach

Hamit *ABDERAMANE*<sup>1,2</sup>, Moumtaz *RAZACK*<sup>1</sup>, and Claude *FONTAINE*<sup>1</sup>

<sup>1</sup>Department of Hydrogeologie UMR 7185, University of Poitiers, France

<sup>2</sup>Departement of Geology, Faculty of Exact and Applied Sciences, University of N'djamena, Chad

Copyright © 2016 ISSR Journals. This is an open access article distributed under the *Creative Commons Attribution License*, which permits unrestricted use, distribution, and reproduction in any medium, provided the original work is properly cited.

**ABSTRACT:** The Chari-Baguirmi aquifer, located East of Lake Chad, is the main source of water in this region. The groundwater piezometry is marked by a large depression. The work presented here aims to understand the development of this depression. The approach is based on a sedimentological study coupled to a hydrogeochemical study of the groundwater. The sedimentological analysis revealed the grain size heterogeneity of the different layers. Clay mineralogy showed that the deposition of sediments takes place from the periphery to the center of the depression. This sedimentation mode suggests the existence of a morphological cuvette to which sediments are driven by the transport agent. We deduced the existence of a "structural" depression unlike the common assumption of an origin due to accentuated evaporation of the groundwater over the depression area. The combined study of chloride and oxygen-18 has shown that the area between Lake Chad and the piezometric depression is a special evaporation zone. This means that the process of evaporation of groundwater does not occur mainly in the center of the depression. The first results of this work provide new insights into the functioning of this important aquifer system and the establishment of the large Chari Baguirmi piezometric depression.

**KEYWORDS:** Lake Chad, Chari Baguirmi aquifer, piezometric depression, structural depression, hydrochemistry, isotopes.

### 1 INTRODUCTION

This work focuses on the study of the Chari Baguirmi groundwater, located East of Lake Chad (Figure 1). The piezometry of this groundwater is marked by a large depression. This kind of depressions in the Sahel region in Africa has been known since the fifties. Several hypotheses have been advanced to attempt to explain the existence of these depressions. The most widely accepted hypothesis suggests the effect of high evaporation of the groundwater at the point of depression (Aranyosy and Ndiaye, 1993).

The study area covers an area of 70,000 km<sup>2</sup>. This work aims to understand the processes that contributed to the establishment of the piezometric depression of Chari Baguirmi (Figure 2), implementing a sedimentological study of the different layers of rocks through the soil surface to the groundwater allowing for a better understanding of the processes of sedimentation, coupled with geochemical and isotopic study of water sampled in the area to understand the processes of mineralization of water and the potential effect of evaporation.

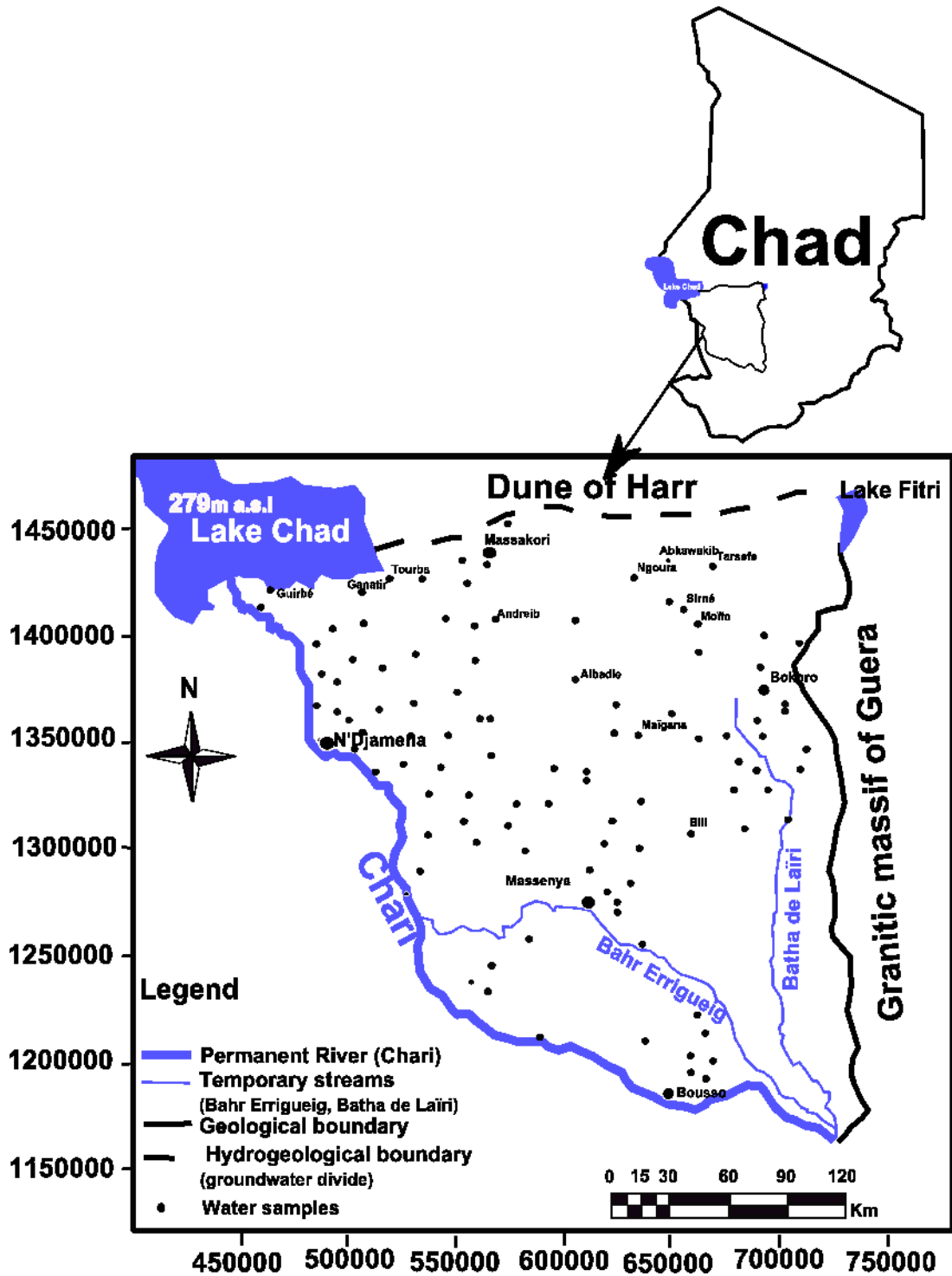


Figure 1. Location of the study area with water sampled points

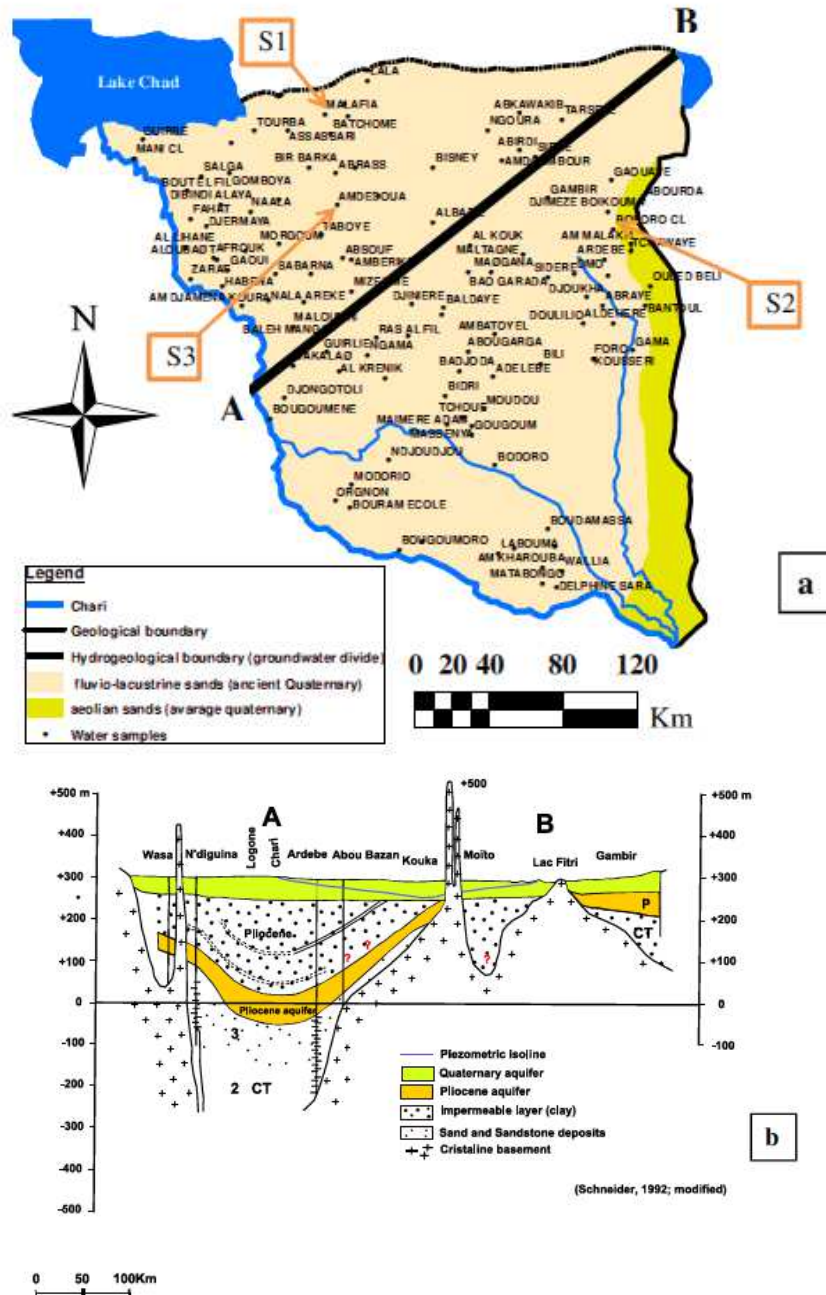


Figure 2. a) Geological map of the study area. b) Geological section along the line AB

## 2 GEOLOGICAL SETTING

The Chari- Baguirmi aquifer system, in the center of the Republic of Chad, is located in the geological basin of Lake Chad (Figure 1), the UTM-33N coordinates are between 450,000 and 750,000 m East longitude and between 1,150,000 and 1,450,000 m North latitude. This area is bounded on the East by the mountains of Guera, on the North by the dunes of Harr, on the West by the Chari River, on the South by the formations of the Continental Terminal and on the Northwest by Lake Chad.

The study area is located in the Sudano-Sahelian zone and receives between 1000 and 400 mm/year precipitation. The average annual rainfall is estimated at 700mm/year. The average monthly temperature is 29.5 ° with maxima between 34° and 43°C and minimum between 17 °C and 23 °C.

The geology of this area has been the subject of several studies due to oil exploration and water drillings carried out in the region. One distinguishes in this area, located on the border of the paleo-chadian basin, three sets with various geological formations that make up the basin and its basement ( Genik 1992; Kusnir and Moutaye 1998; Schneider and Wolf , 1992 and Moussa, 2010) .

- To the Northeast and Northwest, formations of the crystalline basement outcrop in the form of inselbergs at Ngoura , Moïto and Dandi (Figure 3). In general, these are monzogranites , alkali granites and microgranites ( Kusnir , 1995);
- To the center, Pliocene deposits of the paleo-chadian cuvette, cover almost all of the study area. These deposits are represented on the one hand, by a detrital series with predominantly sandy clay intercalations and secondly by a very thick lake sedimentation containing sandy intercalations with gypsiferous clays containing diatomites (Servant - Vildary, 1978).
- Finally Quaternary deposits cover the area by hiding the underlying formations. These Quaternary formations are composed of sandy clastic and clayey sediments, fluvial, lacustrine and deltaic and eolian, that show rapid lateral and vertical facies variations. In the area of Lake Chad (polders of Lake Chad), Carmouze (1975) revealed in the diatomic clayey sediments, the presence of evaporite salts such as gypsum, thenardite , trona, nahcolite etc.

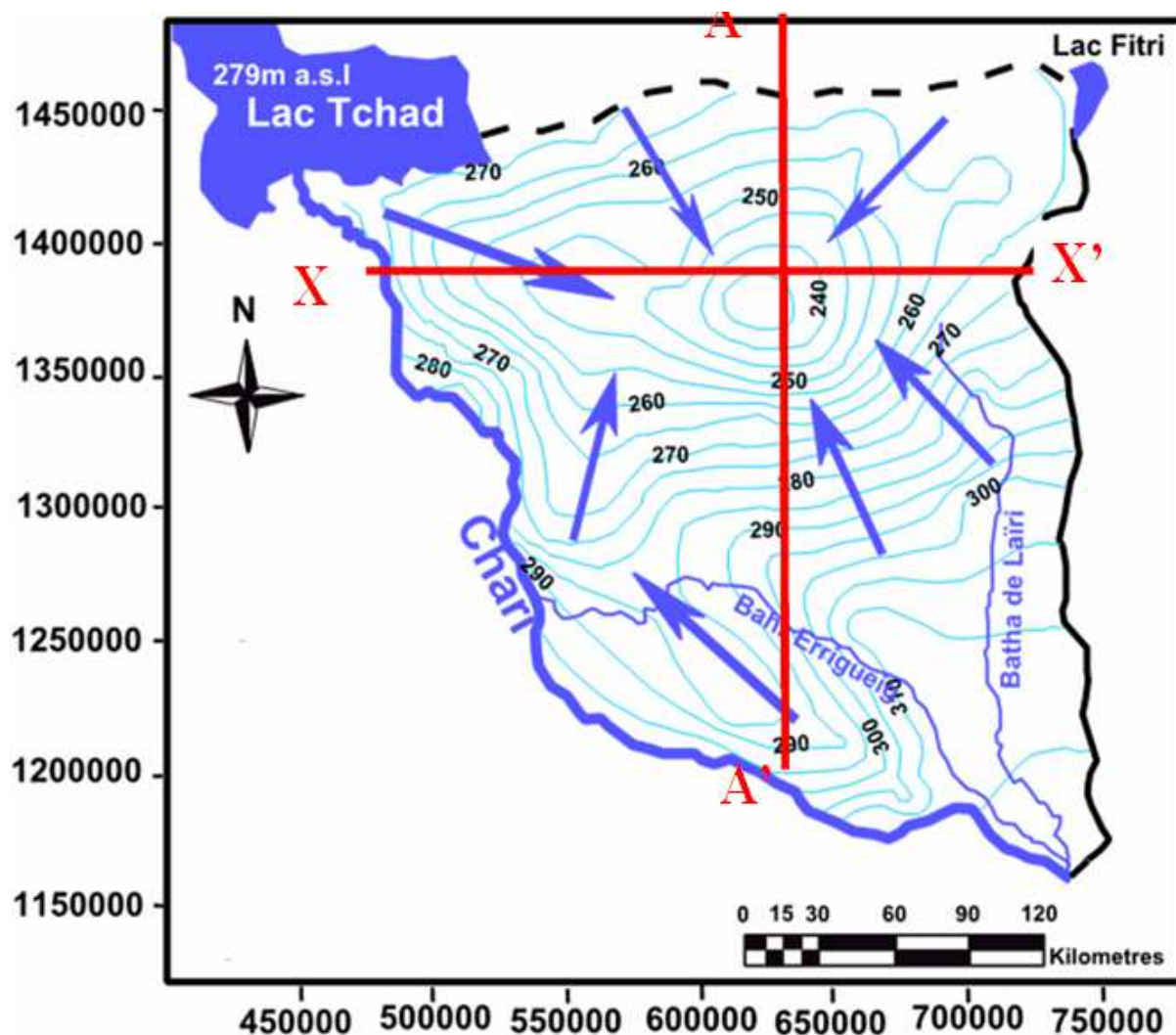


*Figure 3. Map showing the piezometric depression and the profiles along which the study of the groundwater mineralization was made*

### 3 METHODOLOGY

For the sedimentological study (grain size and mineralogy), a sampling of sediments in three wells located respectively to the Northwest, to the East and at the center of the depression was performed (sites S1, S2, S3 - Figure 4). In total 62 samples were collected.

For the grain size analysis, the device is a laser particle sizer of MALVERN Mastersize IP100 brand. It consists of a red laser beam monochromique, an analysis cell containing the slurry and a sensing interferometer. This particle sizer allows obtaining a particle size distribution of the sample.

For the mineralogical analysis, the device is a Xpert PANalytical diffractometer. The semi-quantitative mineralogical analysis using diffraction is based on the proportionality relationship existing between the weight percentage of a phase in a material and the intensity of its major reflection. Among the methods developed, the RIR (Reference Intensity Ratio) is the fastest to implement (Brindley and Brown,1980). In this work, a campaign of piezometric measurements and sampling of groundwater in the Quaternary aquifer were performed on the entire study area (Figure 1). The physico-chemical parameters such as pH, temperature and electrical conductivity were measured *in situ* with a multi-parameters device of WTW Multi 350i brand. Major anions and cations and trace elements were determined by ion chromatography (IC) and emission spectrometry with inductively coupled plasma ICP-OES in the laboratory of BGR (Hannover). Bicarbonates were measured by standard titration methods. The average ion balance for all samples equals 1.55 %. Isotope analyzes of Oxygen-18 and deuterium was carried out at the Laboratory of Applied Geophysics at Leibniz (Hannover, Germany). All samples were measured at least in duplicate and the reported value is the average value. All values are given in standard notation delta per thousand (‰) vs. VSMOW :

$$\delta\text{‰} = ( R_{\text{sample}} / R_{\text{reference}} - 1 ) \times 1000$$

### 4 RESULTS AND DISCUSSION

#### 4.1 GRAIN SIZE STUDY

Three sites were sampled for the grain size study: Malafi well (site S1), Bokoro well (site S2), Amededoua well (site S3). The sediments were collected every meter from the ground surface. A detailed analysis is given below for the well Malafi on site 1, to the West of the depression.

At site 1 (S1) located to the West of the piezometric depression, from 1m to 4m, the sediments consist of sand and silt. One observes (Fig. 4) a layer of silty sand (89% sand, 8% silt) sandwiched between two layers of sandy silt with sand content between 58% and 69% and silt contents ranging from 22 and 30%. After 4m depth, silt content decreases and the sand content reaches about 97%. This layer of sand lies on a 1m thick layer of silty sand (5m to 6m depth) consisting of approximately 82% sand and 12% silt.

From 6m to 10m depth, sand content ranges between 93% and 96%. Then, the sand content falls between 10m and 11 m deep to 58%. Between 11 m and 12m, sand content drops to 18% with a relatively small increase in clay content from 10 % to 13%. This forms a layer of fine silt. Between 12m and 14m deep, there is an increase in sand content reaching 54% and 68%. Between 14m and 15m depth, sand content increases (84%) to form a layer of silty sand. Finally, beyond this depth till the watertable which is at a depth of 17m, there is a gradual increase in sand content up to 96%.

On sites no.2 and 3, we find this alternating sediments of different size (sand, silt,...) with varying thicknesses.

The above demonstrates the existence of a layer transition which results on the profile by an oscillation of the vertical permeability from the surface to the depth indicating a noticeable vertical permeability heterogeneity.

Depth (m)	% Sands	% Clay	% Silts	Lithology	Description
1	69	9	22		Sandy silts
2	89	3	8		Silty sands
3	58	13	29		Sandy silts
4	97	1	2		Sands
5	82	6	12		Silty sands
6	94	2	4		Sands
7	94	2	4		
8	95	1	4		
9	95	2	3		
10	96	1	3		
11	58	10	32		Silty sands
12	18	13	69		Silts
13	68	5	27		Sandy silts
14	54	10	36		
15	84	3	13		Silty sands
16	95	1	4		Sands
17	96	1	3		

Figure 4. Granulometric and geological cross-sections of the site S1 (depths from 1m to 17m)

#### 4.2 MINERALOGICAL STUDY

A first set of analyzes focused on the entire sediment prepared by grinding in agate mortar. For almost all materials, the essential component is quartz (Fig. 5). It follows that the other components are often poorly or not detected. Consequently, for reasons of better mineralogical information, our attention was focused on the silty clay fraction (<50microns) to better understand the deposition conditions and evolution of these materials.

Within this fraction (<50 microns), the particle size of fine silt (20-2 microns) is still dominant (55 to 57% in average). However, the clay fraction (<2 microns) can sometimes be also abundant.

The class of coarse silt (50 - 20µm) is still a minority (on average 15 to 16% in series 1 and 2, but only 10% in the series 3). It is best shown in series 1 and at the top of the series 2. It is very low in the lower part of the series 3. However, the observation of the evolution of this class shows some cyclicity along the log of the series 3 with maximum respectively located at 8, 14, 21, 25, 34 and 40 m.

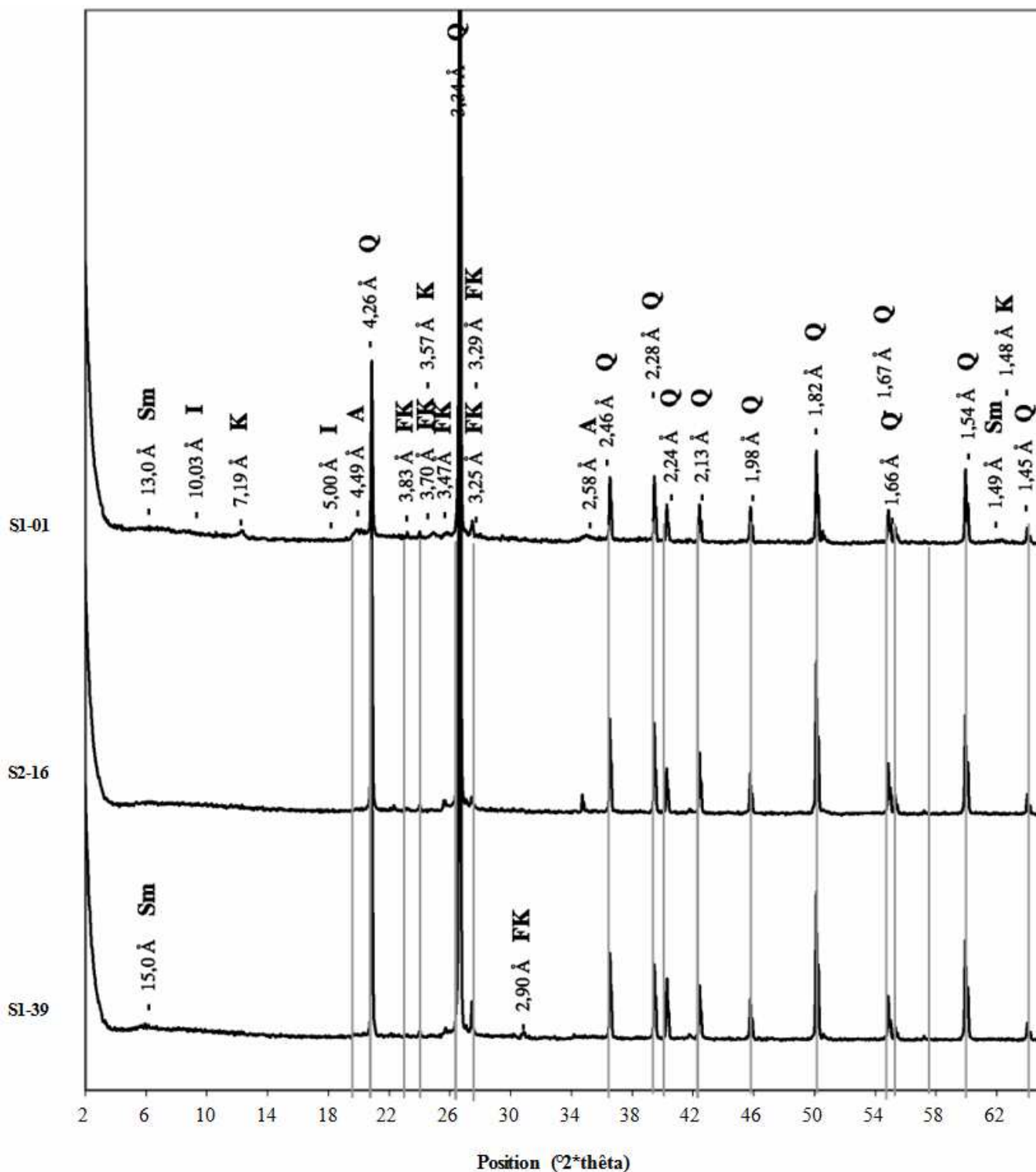


Figure 5. Examples of diffractograms of the whole sediment sample: S1-01, S2- 16 and S3-39. Clays (A), smectite (Sm), illite (I), kaolinite (K), quartz (Q), K feldspar (FK).

**A) MINERALOGY OF THE TOTAL FRACTION <50 MICRONS**

Although this fraction of <50 microns represents sometimes relatively small proportions of the sediment, it has the advantage of showing more varied mineralogical species (Fig. 6), which allows a greater number of mineralogical information.

Indeed, one detects a detrital procession composed mainly of quartz, usually associated with small amounts of potassium feldspar (orthoclase or microcline) and, more rarely, plagioclase, and an assemblage of clay minerals composed of smectite, kaolinite and illite. With the exception of plagioclase, these minerals are found in all sedimentary levels. Other minerals, such as calcite, goethite, and gypsum appear more punctually.

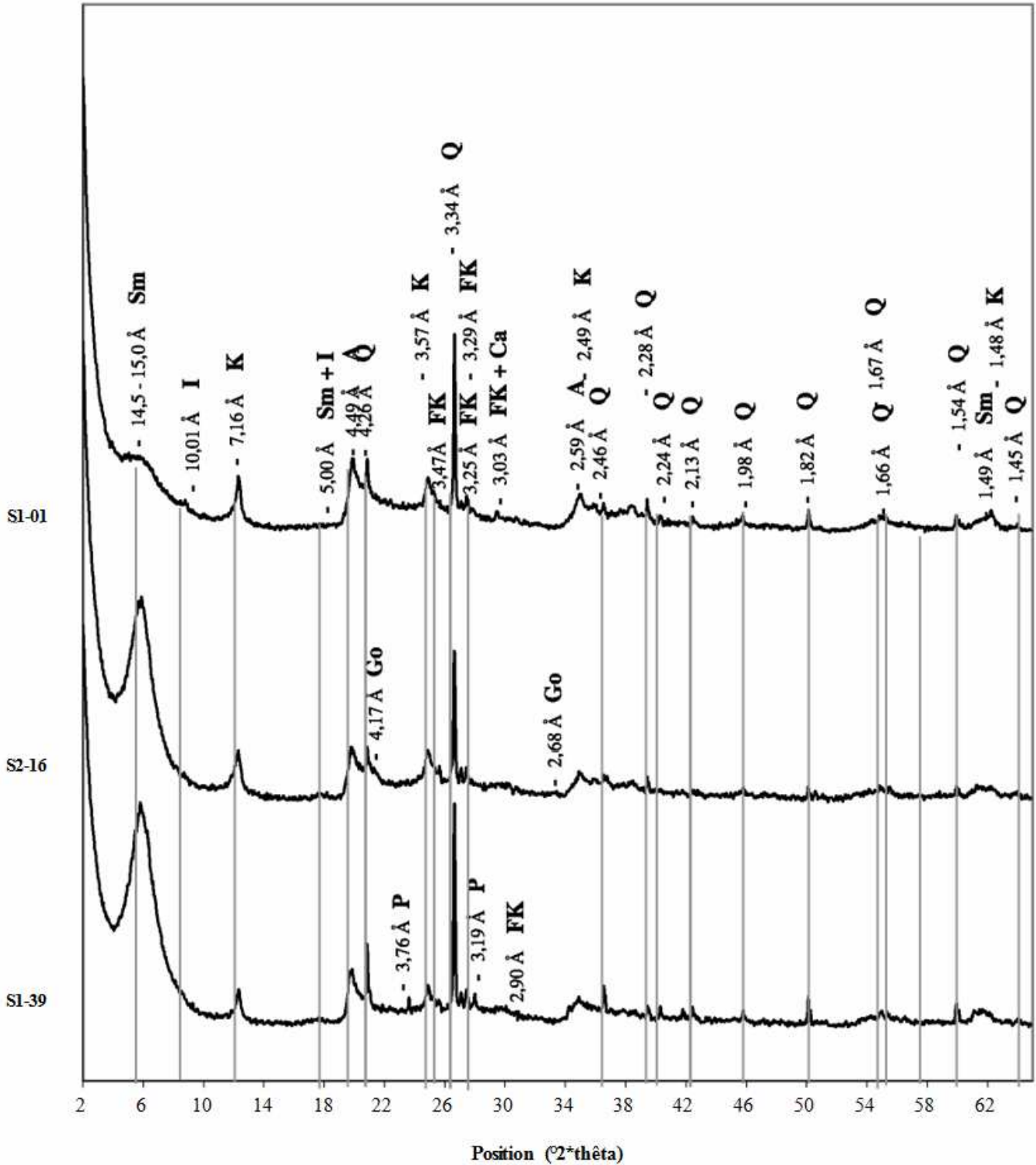


Figure 6. Example of diffractograms of the fraction <50 microns: samples S1- 01, S2-16 and S3-39. Plagioclase (P), Goethite (GB), Calcite (Ca).

**B) MINERALOGY OF THE CLAY FRACTION <50 MICRONS**

The clay minerals were determined from the diffraction patterns of oriented preparations first air-dried and glycol by the spray method (Fig. 7). Only three clay phases have been identified: smectite, kaolinite and illite. A further study by deconvolution of diffractograms of powder of the fraction <50 microns shows that, overall, the smectites belong to the montmorillonite-beidellite family of series of dioctahedral smectites.

The deconvolution method applied to the diffractograms of oriented glycol preparations has also identified crystallographic criteria related to the crystalline organization of the clay minerals. For each clay species, the number of sheets in the stack base was calculated. Regarding the smectites, the analysis was completed by calculating the index of Biscay (IB) (Biscay 1965).

Of all the samples studied, smectites have a number of sheets in the stack extremely constant, between 16 and 17. The distribution of the IB of the smectites of series 1 (Fig8) clearly shows the existence of two populations: one (A) between 0.0 and 0.3 and the other (B) between 0.4 and 0.6. The population A is close to 65% of the smectites found in the levels studied in this series.

In series 2, however the population B ( $0.4 < IB < 0.6$ ) is largely dominant and A population represents only 12.5% of total smectites. In the three series (Fig. 9), smectites show a moderate ( $IB = 0.4$  to  $0.6$ ) to well crystallized ( $0.6$  to  $0.8$ ) population. This increase in crystallinity is particularly clear if we consider on the one hand the series S1 and on the other hand the series S2 and S3. In addition, a population of low crystallinity ( $IB = 0.1$  to  $0.3$ ) has been identified in the only series S1. Holders of this population of low crystallinity alternate with those of the population of higher crystallinity, without showing a crystallinity gradient with depth. Illite crystallinity is determined based on the number of sheets in the stack (Fig.10). If the distribution is quite spread in the S1 series, it is narrower and symmetrical for S2 and S3 series. For this reason, the median is the most characteristic statistics of illite populations. From S1 to S3 series (Fig. 11), there is a marked decrease in the number of sheets in the stack, with a decrease of almost one third.

The crystallinity of kaolinite was also followed by observing the changes in size of the coherent domain. It appears (Fig.12), that the distribution of the number of sheets in the stack is reduced in the vicinity of 140 in Series 2, but more spread out for series 1 and 3. If there is a slight difference in the number of sheets stacked between these three series (Fig.13), there is no clear trend to a gradual decline from series 1 to series 3, as was highlighted for illite.

The reverse evolution of the size of the coherent domain of illite and smectite could be explained by different modes of formation, such as detrital contribution, neof ormation in more or less humid soil profiles, crystallization in lacustrine or fluvio-lacustrine environment in semi-arid climate.

In the case of kaolinite, its contents appear generally slightly larger ( $> 10\%$ ) in the upper part of the three series. But there is no distinct change in its crystallinity, to the north or south of the study area.

The semi-quantitative analysis of the total fraction < 50 microns shows that this fraction is essentially constituted by a procession of clay minerals associated with quartz. These two components generally account for two three quarter of this fraction with an average of 43 to 45% for one and 34 to 36 % for the other respectively. Feldspars associated with quartz are microcline (KAlSi<sub>3</sub>O<sub>8</sub>) and plagioclase (albite NaAlSi<sub>3</sub>O<sub>8</sub> essentially).

The carbonates are found mainly in the S1 series. They are usually calcite (CaCO<sub>3</sub>), sometimes accompanied by dolomite ([Ca, Mg] [CO<sub>3</sub>]<sub>2</sub>). In other series (S2 and S3), carbonates are minor or trace, and appear only very occasionally.

An iron oxide, goethite (FeOOH) was specifically detected in the sequences of the northern study area (series S1 and S2). It appears in small amounts (a few percent) in the lower horizons of the series, where its presence marks phenomena of ferruginisation. No iron oxide was identified in the S3 series.

Finally, gypsum (CaSO<sub>4</sub>, 2H<sub>2</sub>O) was identified at 3 m deep in the S1 series. This is the only sulfate clue encountered in all samples studied. The procession of clay minerals is thus formed in the following order, smectite, kaolinite and illite. From series S1 to S3, the content ratio evolves as follows: 42:5:3 → 44:4:2 → 45:3:1. If the smectite phase is still dominant, its participation becomes even more important when moving from north to south, and that as well at the expense of illite than kaolinite. This is also very noticeable relationship with depth. Indeed, the levels of the upper part of each of the three series are systematically richer in illite and kaolinite than the lower levels. Should we see a change in the conditions of implementation of these minerals from more wetlands to more arid environments in recent times? These changes are, however, sufficiently moderate as smectites are still of dioctahedral type. This is in contrast to what is happening in the South of the depression of Lake Chad, in the drainage area of the Logo and Chari rivers, where the newly formed trioctahedral smectites of stevensite type and saponite has been demonstrated (Carmouze et al, 1975).

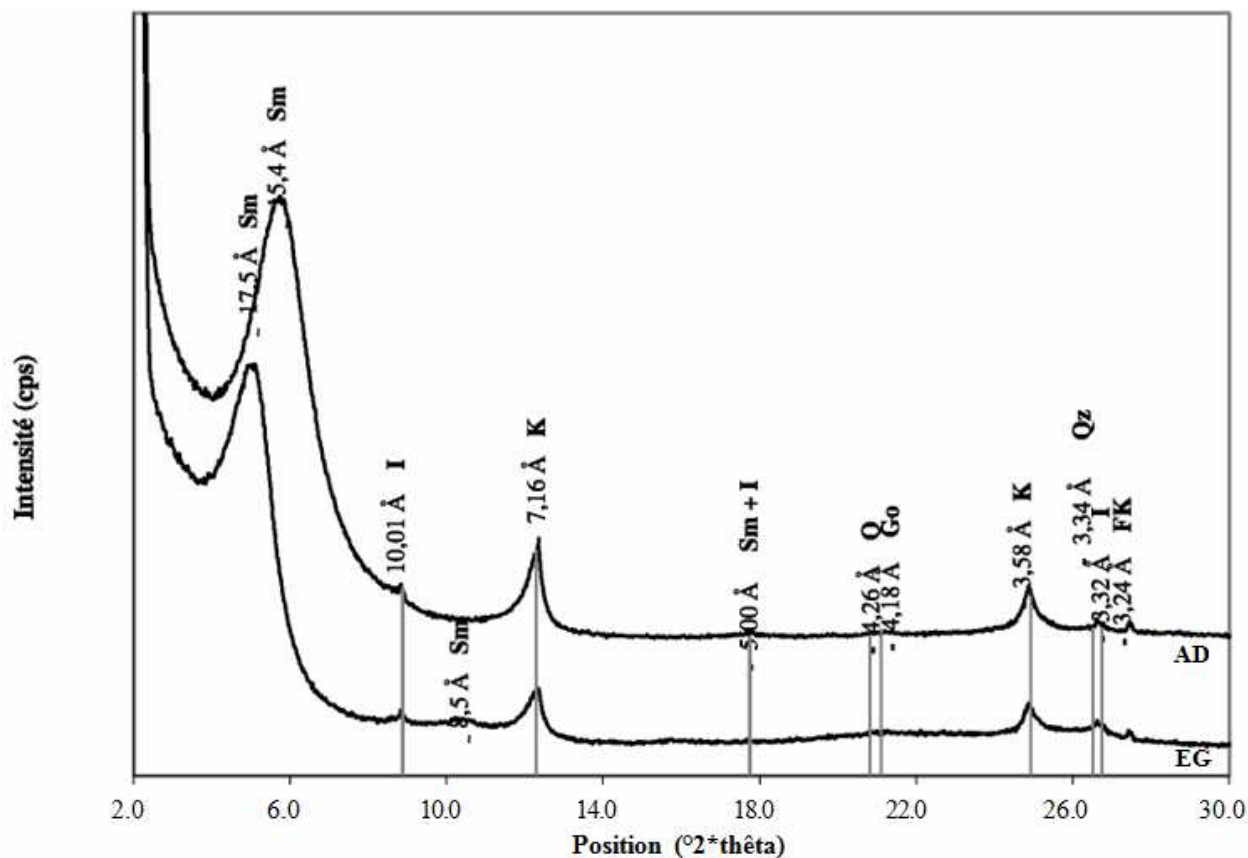


Figure 7. Behavior of clay minerals in the fraction <50 microns of sample S2-16 after drying (AD) and glycolage (EG). (Smectite Sm; Illite: I, Kaolinite: K; Quartz: Qz; Feldspar K: FK; Goethite: GB).

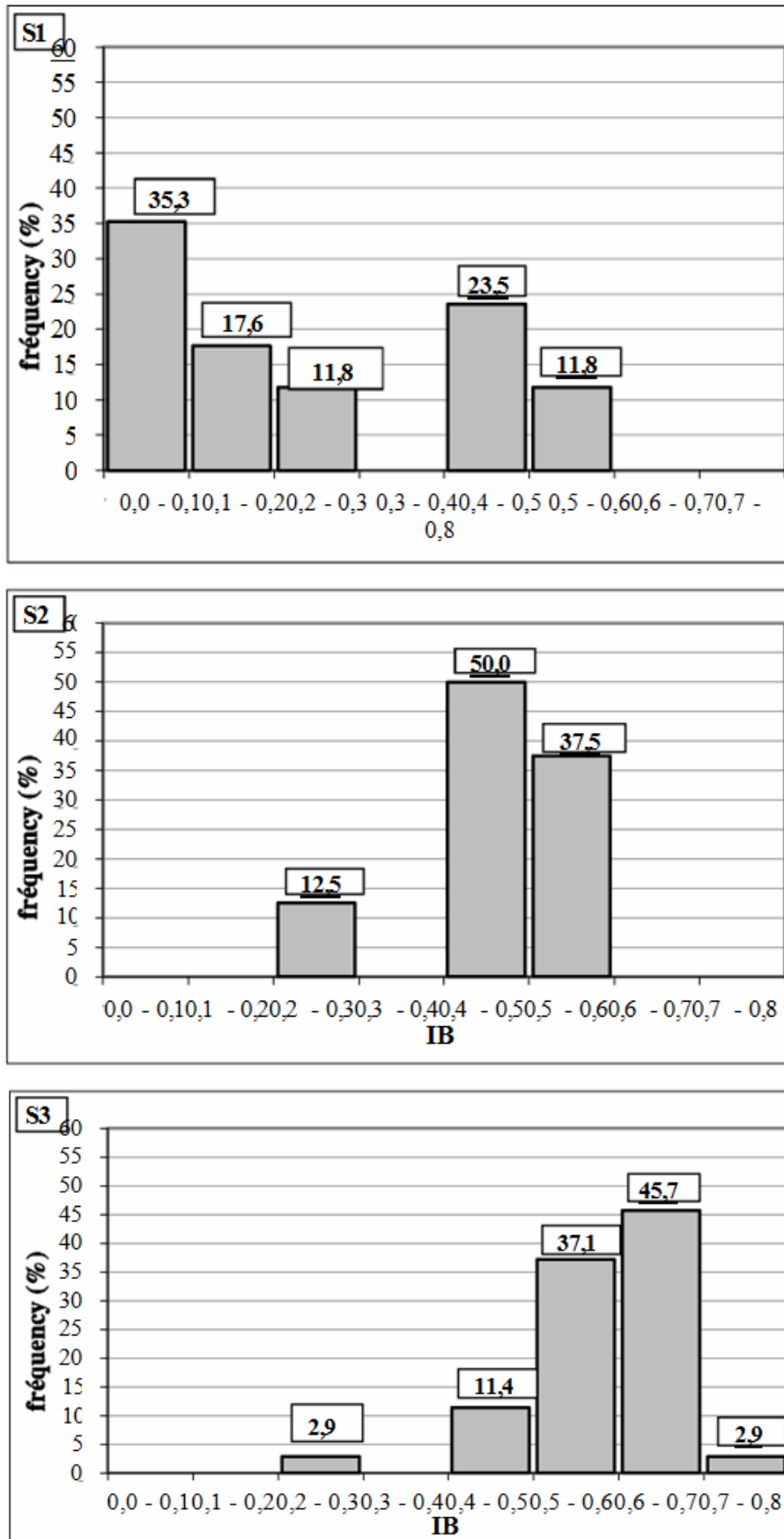


Figure 8. Index of Biscaye (IB) distribution of smectites in the sedimentary series at sites S1, S2 and S3.

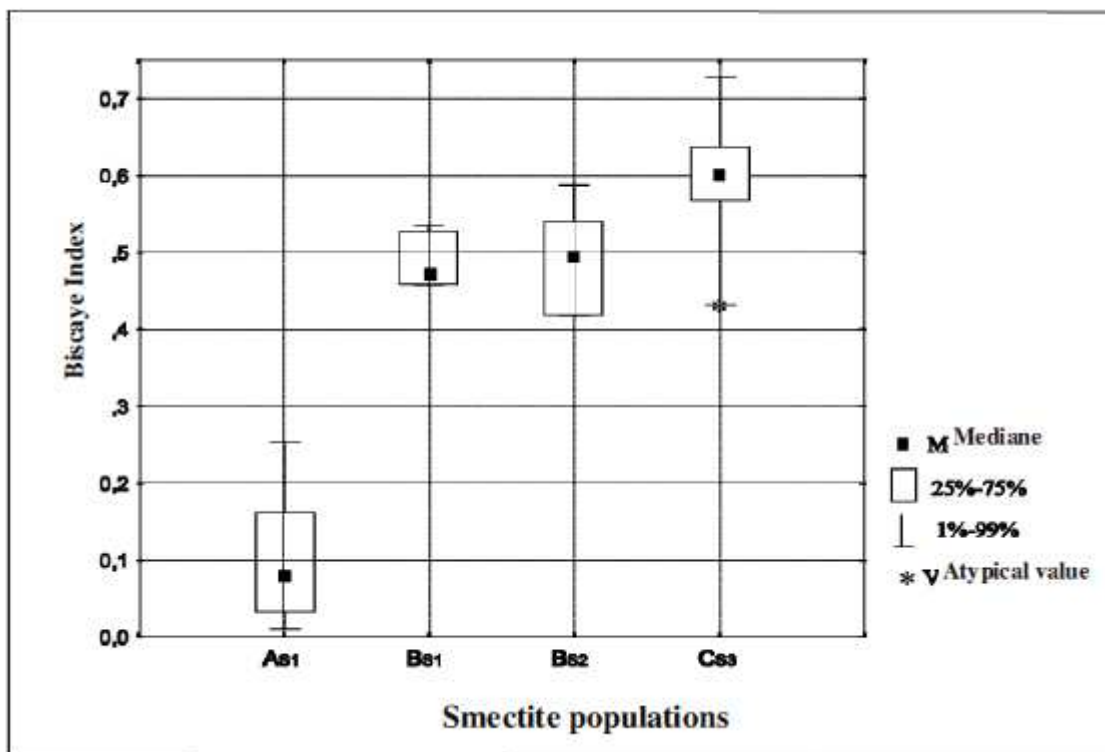


Figure 9. Statistical characteristics of the populations of smectite (A, B and C) identified in the sedimentary sequences S1, S2 and S3 from Biscaye index distributions.

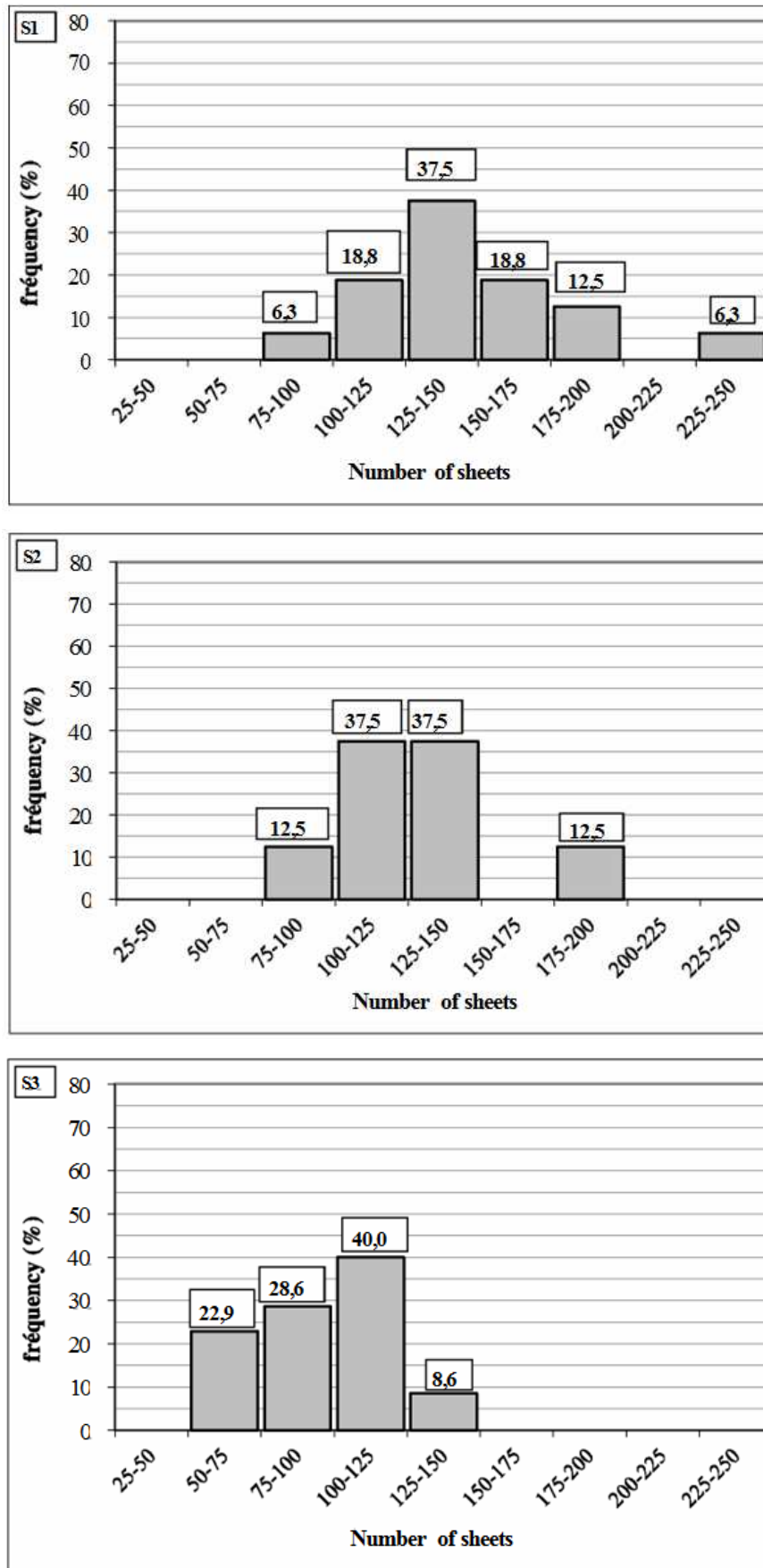


Figure 10. Distribution of the Illite number of sheets in the sedimentary series at sites S1, S2 and S3

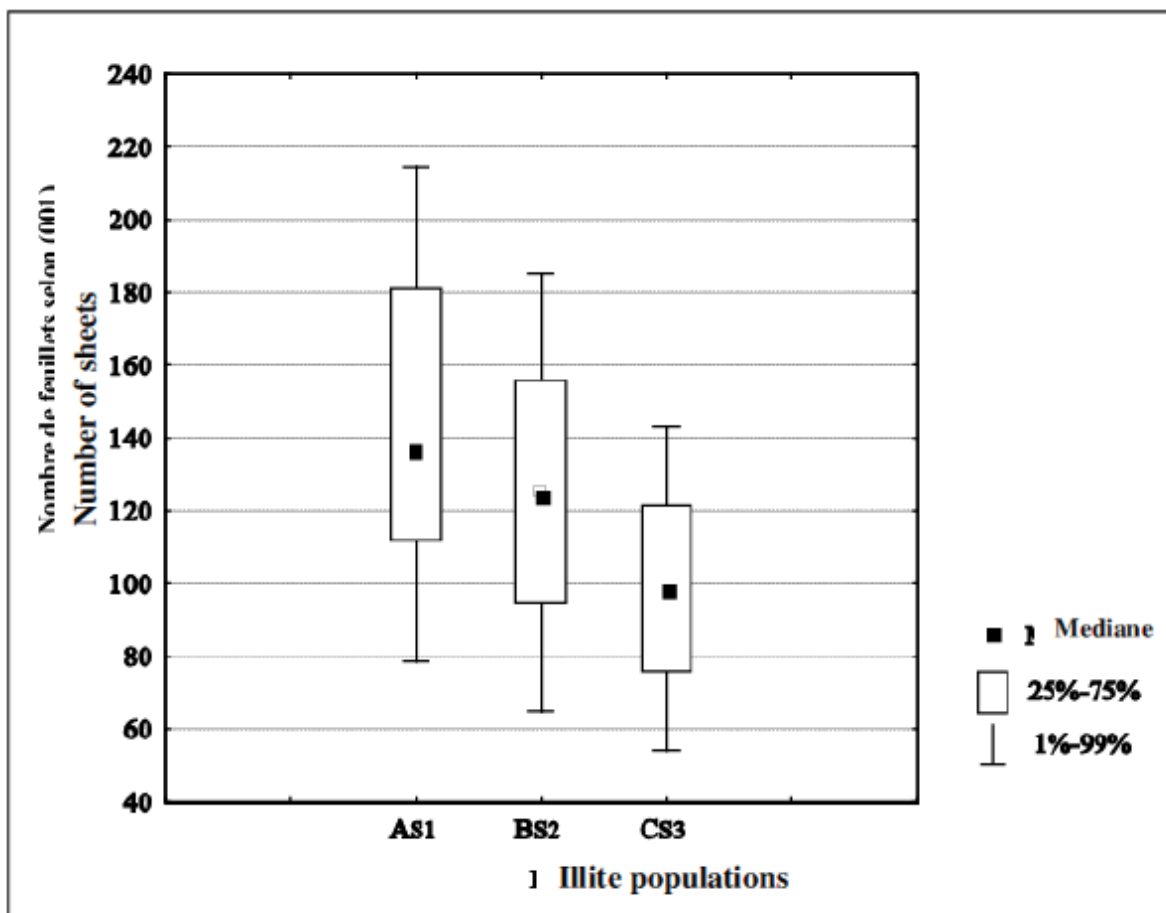


Figure 11. Statistical characteristics of the illites populations (A, B and C) identified in the sedimentary sequences S1, S2 and S3 based on the distributions of the number of sheets in the stack

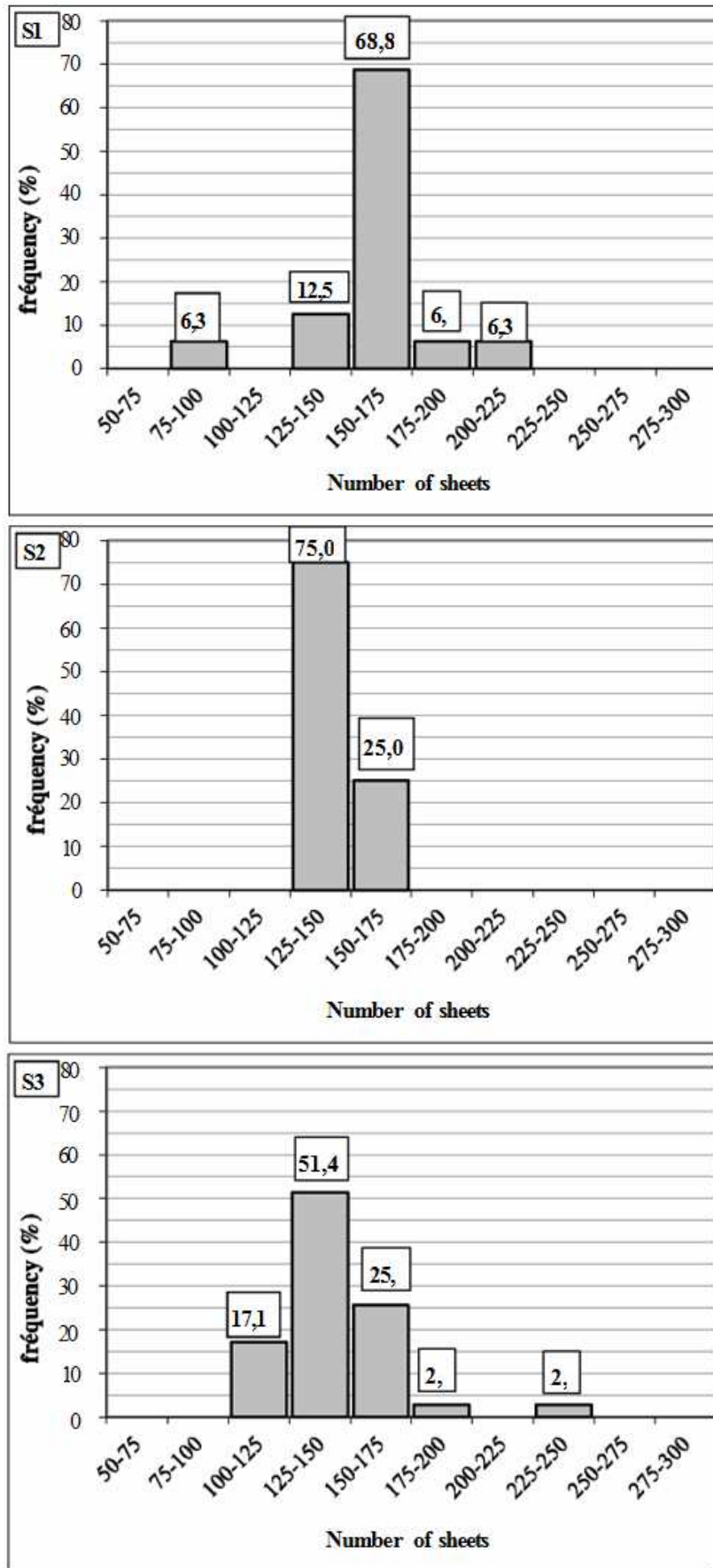


Figure 12. Distribution of the Kaolinite number of sheets in the sedimentary series at sites S1, S2 and S3

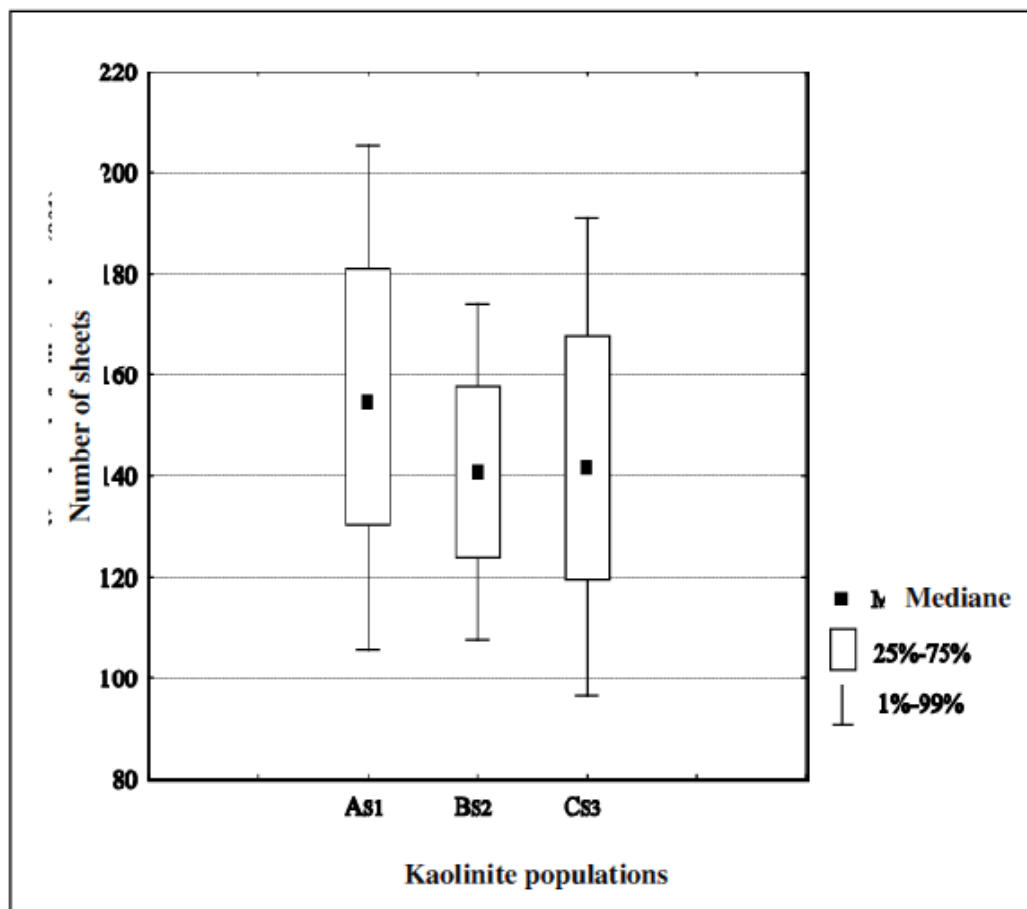


Figure 13. Statistical characteristics of the kaolinite populations (A, B and C) identified in the sedimentary sequences S1, S2 and S3 based on the distributions of the number of sheets in the stack.

#### STUDY OF THE GROUNDWATER MINERALIZATION FROM NORTH TO SOUTH ALONG THE PROFILE AA'

The majority of samples along the profile have a conductivity less than 400  $\mu\text{S}/\text{cm}$ . The highest measured value is 2620  $\mu\text{S}/\text{cm}$ . The lowest conductivities are observed South of the depression and the highest in the North of the depression. The values are low in the South as the ETP (Potential EvapoTranspiration) is also low in this part of the study area as seen above. They are high in the North, given the ETP is about 2000mm/year. Indeed, evaporation increases the content of dissolved salts by reducing the volume of water to saturation vis-à-vis a given mineral.

If we consider the oxygen-18 isotope and  $\text{Cl}^-$  ion as a conservative element (Fontes et al, 1969) to study the acquisition of groundwater salinity, the content of  $\text{Cl}^-$  in rainwaters compared to the groundwater gives an estimate of the concentration factor by evaporation. This, provided no source of chlorides other than meteoric input is considered.

The study of the salinity distribution along the profile AA' (Fig. 14) shows that the acquisition of salinity does not obey the centripetal gradient in accordance with what one would expect from an internal drainage. The mode of acquisition of groundwater salinity is governed by the dissolution of evaporite formations (gypsum, thenardite etc.) around Lake Chad, associated in the downstream part, with evaporation from the border of the lake to the center of the depression. The graph of  $\delta^{18}\text{O}$  vs.  $\text{Cl}^-$  following the profile AA' shows that the water can be divided into three groups: (1) a set of water collected on the border of Lake Chad, enriched and not evaporated, (2) a set of water taken between the border of Lake Chad and the center of the depression un-enriched and evaporated and (3) a homogeneous mass of water from the mixing of these waters with waters collected South of the depression marked by a process of base exchange.

The evolution of the groundwater hydrochemical properties from North to South and partly from West to East, towards the depression, is characterized firstly by dissolution of gypsiferous formations associated with evaporation, and secondly, by base exchange process. Isotopic properties identify evaporation as a process of concentration of ions.

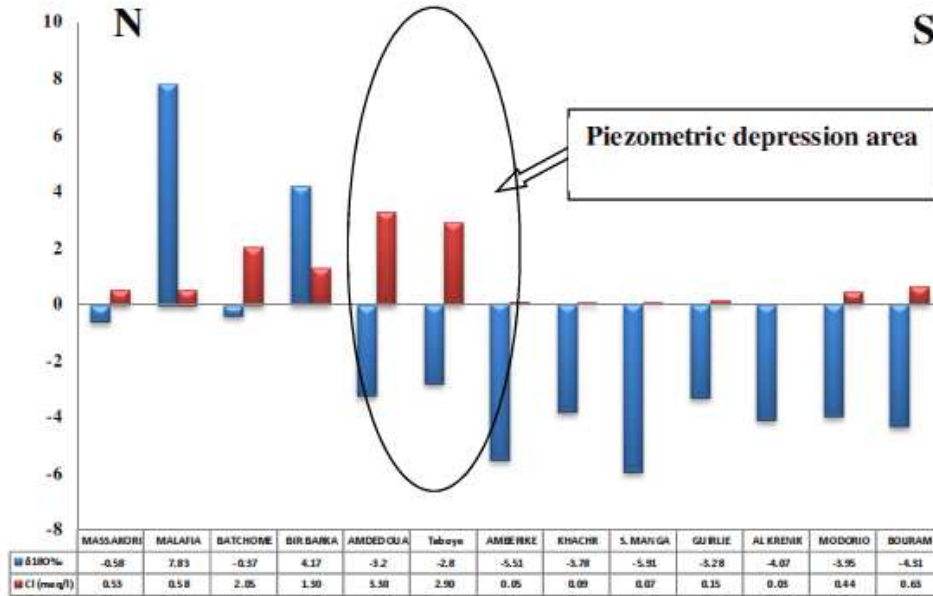


Figure 14. Relationship between the chlorides contents and 618O of Chari Baguirmi groundwater. Evolution from North and from South to the center of the depression.

**STUDY OF THE GROUNDWATER MINERALIZATION FROM WEST TO EAST ALONG THE PROFILE XX'**

The study of the mineralization of the waters along the profile XX' (Fig. 15 ) shows that the acquisition of the salinity obeys the centripetal gradient , in accordance with what one would expect from a internal drainage. Indeed, as the depression is the outlet, the mode of acquisition of groundwater salinity is governed by the mixing of waters in the center of the depression.

The graph representation of  $\delta^{18}O$  vs. Cl following the profile XX' shows that the water can be divided into two groups: (1) a group of water collected either South or West of the depression, with an evaporated and not enriched characteristics (2) a group of water taken in the depression consisting of a mixture of water.

The salt content is mainly due to the dissolution of gypsiferous formations and concentration by evaporation of solutions, highlighted by the study of  $\delta^{18}O$  and chloride contents. The study of the mineralization along these two profiles shows that the process of evaporation of groundwater does not occur at the center of the depression but rather to the West of the depression in an area between Lake Chad and the depression.

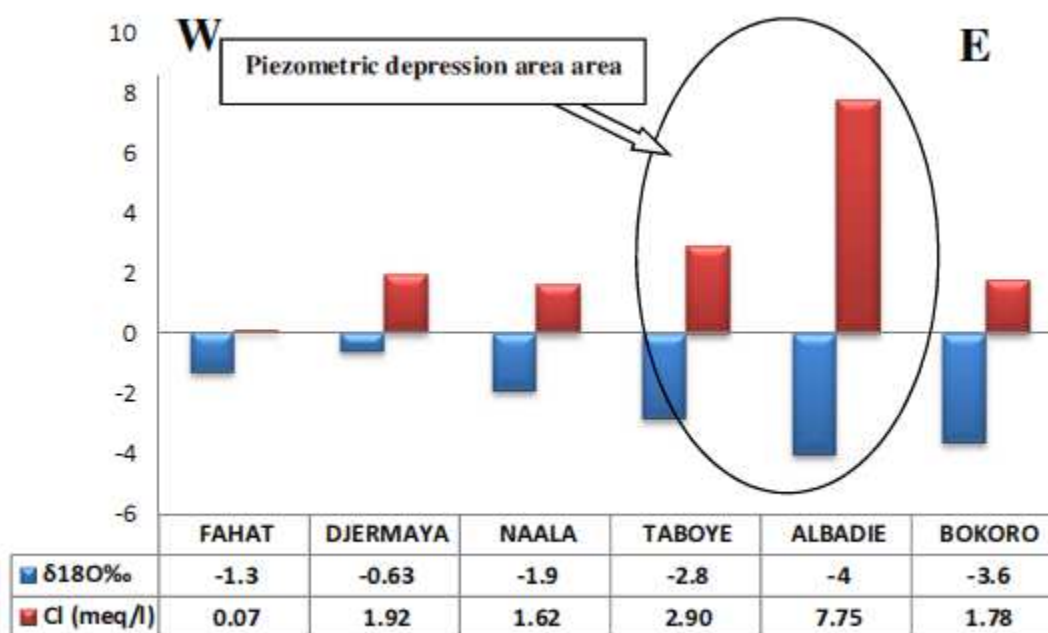


Figure 15. Relationship between the chlorides contents and  $\delta^{18}O$  of Chari Baguirmi groundwater. Evolution from West and from East to the center of the depression

## 5 CONCLUSION

The sedimentological analysis of the different layers of rock encountered up and down in the wells, allowed to highlight the grain size heterogeneity of the different layers. The analysis of clay mineralogy has shown that the deposition of different sediments occurred from the periphery to the center of the depression. This mode of sedimentation suggests the existence of a structural cuvette (depression) to which sediments are driven by the transport agent.

The existence of a "structural" depression contradicts the usual hypothesis of formation of these depressions due to high evaporation. In addition, the presence of a thick clay layer observed in the depression does not support the hypothesis of high evaporation of the groundwater. The hydrochemical and isotope study based on the relationship Cl versus  $\delta^{18}O$  showed that the initial isotopic composition has been modified by the evaporation of rainwater during infiltration. This led to a mixture of water of different isotopic signatures. It shows that the mineralization process and the origin of the salinity in the center of the depression are related on one hand to the lithology, on the other hand, to climate phenomena causing evaporation of water from the aquifer. This work thus provides new insights into the functioning of this important aquifer system and the establishment of the piezometric depression of Chari Baguirmi.

## REFERENCES

- [1] **Aranyossy, J. F. et Ndiaye, B., 1993.** Étude et modélisation de la formation des dépressions piézométriques en Afrique sahélienne. Analysis and modeling of the piezometric depressions in Sahelian Africa. In French. *Revue des sciences de l'eau / Journal of Water Science*, vol. 6, n° 1, 1993, p. 81-96.
- [2] **Biscaye, P.E., 1965.** Mineralogy and sedimentation of Recent deep-sea clay in Atlantic Ocean and adjacent seas and oceans. *Geological Society of America Bulletin*, 76, 803-831.
- [3] **Brindley G.W., and Brown G. 1980.** Crystal structures of clay minerals and their x-ray identification. Mineralogical Society, Monograph n°5, London, 495 p.
- [4] **Brindley G.W., and Udagawa S., 1960.** High-temperature reactions of clay mineral mixtures and their ceramic properties. *Journal of American Ceramic Society*, 43, 59-65.
- [5] **Carmouze, J.P., Cheverry, C., Gac, J.Y., Maglione, G., et Roche, M.A., 1975.** Aspects sédimentologiques actuels d'un bassin continental endoréique : le bassin tchadien. Current sedimentological aspects of continental endorheic basin: the Chad basin. In French. . 9th International Congress of Sedimentology, Nice France). 9 p

- [6] **Fontes, J.C., Moglione, G., et Roche, M.A., 1969.** Données isotopiques préliminaires sur les rapports du lac Tchad avec les nappes de la bordure Nord-Est. Preliminary data on isotopic ratios of Lake Chad with the groundwater of the North-East border. In French. Cahier de l'ORSTOM série hydrologie, 6(1) : pp.17-34.
- [7] **Genik, G.J., 1992.** Régional framework structural and petroleum aspects of rift basins in Niger, Chad and Central Africa Republic (C.A.R). Tectonophysics, 213: 169-185.
- [8] **Klug, H.P. et Alexander, L.E., 1974.** X-ray diffraction procedures for polycrystalline and amorphous materials. 2nd editio, Wiley (New York), xxv, 966 p.
- [9] **Kusnir, I., 1995.** Géologie, ressources minérales et ressources en eau du Tchad. Geology, mineral resources and water resources in Chad. In French. Travaux et documents scientifiques du Tchad. Connaissance du Tchad I., 100p.
- [10] **Kusnir, I., et Moutaye, H.A., 1998.** Mineral Resources Chad: a review. Journal of African Earth Sciences, 24(4):549-562.
- [11] **Moussa, A., 2010.** Les séries sédimentaires fluviatiles, lacustres et éoliennes du bassin du Tchad depuis le Miocène terminal. Sedimentary fluvial, lacustrine and eolian series of the Chad Basin since the Miocene. In French. PhD thesis. Univ.of Strasbourg.
- [12] **Schneider, J.L., and Wolf, J.P., 1992.** Carte géologique et carte hydrogéologique au 1/1500000 de la république du Tchad. Geological and hydrogeological map at 1/1500000 of the Republic of Chad. Ed. BRGM. Orléans, France.
- Servant-Vildary S., 1978.** Etude des diatomés et paléoclimatologie du bassin tchadien au Cénozoïque supérieur. Study of diatoms and paleoclimatology of Chad Basin during Upper Cenozoic. In French. Travaux et documents O.R.S.T.O.M. N° 84. 346p.